Doi: 10.31276/VJSTE.61(3).25-32

Characterization of optical parameters of breast cancer cell line - BT474 by polarimetry technique

Thanh-Truc Nguyen[1], Minh-Vy Huynh[1], Thanh-Hai Le[2], Thi-Thu-Hien Pham[1*]

[1]Department of Biomedical Engineering, International University, Vietnam National University, Ho Chi Minh city
[2]Faculty of Mechanical Engineering, University of Technology, Vietnam National University, Ho Chi Minh city

Received 11 December 2018; accepted 25 March 2019

Abstract:

Breast cancer is a well-known health issue that has been a major focus for healthcare professionals for quite some time. Still, the most common noninvasive diagnostic tool - mammography - results in a high false positive rate along with risks of exposure to radiation. These disadvantages are magnified and become more severe when screenings are done repeatedly. To tackle this problem, we introduce a novel framework for uncomplicated diagnosis of breast cancer. Our method utilizes the analytical technique of Mueller matrix decomposition and Stokes vector polarimetry from a polarized light system consisting of a helium-neon laser (wavelength of 632.5 nm), a quarter-wave plate, polarizers, and a Stokes polarimeter. Thus, this technique introduces no radiation. We extracted nine optical parameters of a breast cancer cell line - BT474 - and determined the relationship and separation power of these parameters to cancerous cells and healthy cells. Specifically, the samples were designed as a two-dimensional cellular model of malignant breast tumours that combined a range of four cell densities - 10^4, 10^5, 10^6, and 10^7 cells - per an area of 9 cm^2. Nine optical parameters - orientation angle of linear birefringence (α), retardance or linear birefringence (β), optical rotation angle or circular birefringence (γ), orientation angle of linear dichroism (θd), linear dichroism (D), circular dichroism (R), degrees of linear depolarization (e1 and e2), and degree of circular depolarization (e3) - were extracted from a total of 40 samples using the polarized light system. The results revealed the positive correlations between three cell densities (10^4, 10^5, and 10^6) and the orientation angle of linear birefringence ($R^2 = 0.8038$), linear birefringence ($R^2 = 0.8627$), and linear dichroism ($R^2 = 0.9662$). Meanwhile, both the orientation angle of linear dichroism and circular dichroism illustrated the negative correlation with that range of cell densities with $R^2 = 0.9983$ and 0.9447, respectively. This proves that the optical parameters measured demonstrate significant association with the cells' characteristics and thus, the proposed method could pave the way for an accessible diagnosis of breast cancer.

Keywords: **breast cancer cell line, BT474, circular birefringence, linear birefringence, linear dichroism, Mueller matrix decomposition, optical properties, polarized light, Stokes polarimeter.**

Classification number: **2.3**

Introduction

Breast cancer, which takes place when cells in the breast begin to grow uncontrollably, has developed into one of the major public health problems worldwide, with 50-80% of breast cancer cases being invasive ductal carcinoma. In spite of being the gold standard among diagnostic tools, conventional imaging examinations (i.e., X-ray mammography, ultrasonography, and magnetic resonance imaging - MRI) have their disadvantages. In fact, X-ray mammography has been reported to have low sensitivity and specificity [1-3]. To overcome low accuracy and limited availability of breast cancer diagnostics, various optical techniques have recently been proposed for screening breast cancer, including near-infrared optical tomography, optoacoustic imaging, Raman spectroscopy, diffuse optical spectroscopy, time-resolved diffuse optical spectroscopy, and polarized light. Their advantages in comparison with the standard techniques are enhanced accuracy, speed, and cost-effectiveness. Additionally, due to their simple facilities, they are more suitable for continuous bedside monitoring.

Polarized light, a different dimension of biomedical photonics, has offered new possibilities for noninvasively diagnostic approaches. Recently, various methodologies have been proposed for determining the optical properties of turbid media. To date, the polarized light method has been applied successfully to investigate optical properties of

*Corresponding author: Email: ptthien@hcmiu.edu.vn

several types of biological and pathological samples, such as collagen components [4, 5], diabetes [6], cancer [7], and partial bladder outlet obstruction [8]. Pham, et al. proposed the decoupled analytical technique to extract nine effective optical parameters of turbid media utilizing Mueller matrix decomposition and Stokes vector polarimetry [9-11]. This method determined Mueller matrices of the parameters in a decoupled manner [9]; hence, it could reduce error as well as solve the problem of multiple solutions in previous works. Additionally, the technique was successful in extracting the full polarization properties of a turbid medium in one measurement [10, 11].

The challenges of applying polarized light in screening for cancer include the method of extracting full-range optical values of the biological samples, data bank building, and early detection when malignant cells are in low density. The process of collecting pathological tissues for building a data bank has limitations, as cancerous tumours could be polyclonal [12], various in types and grades [13], and present in a finite supply. In this work, we apply Mueller matrix decomposition and Stokes vector polarimetry to screening for breast cancer. This method is a novel technique using polarized light to solve the problem of extracting full-range optical parameters. Meanwhile, there was no report on utilizing Mueller matrix decomposition to investigate breast cancer. The research was expected to provide a measurement range of the optical system and effective parameters of a mammary carcinoma cell line - BT474. That investigation would be useful for the optical system upgrade, the understanding of cancer-light interaction, and the building of a data bank for breast cancer detection through sample taxonomy.

The samples used in the research were two-dimensional cellular models of breast cancer. The cell line was BT474. In histological taxonomy, BT474 is derived from invasive ductal carcinoma, which accounts for 50-80% of breast cancer types [14]. In molecular classification, BT474 is in luminal B, one of five subtypes, with the expression of the estrogen receptor (ER), progesterone receptor (PR), and human epidermal growth factor receptor 2 (HER2) [15].

Methodology

Optical system set-up and measurement

The technique applied in the research was Mueller matrix decomposition and Stokes vector polarimetry. Fig. 1 illustrates the schematic of the optical system. Nine effective parameters can be extracted for each sample. Table 1 presents names, symbols, ranges, and the formulas for nine effective parameters. More details about the technique can be found in the previous work of Pham and Lo [9-11].

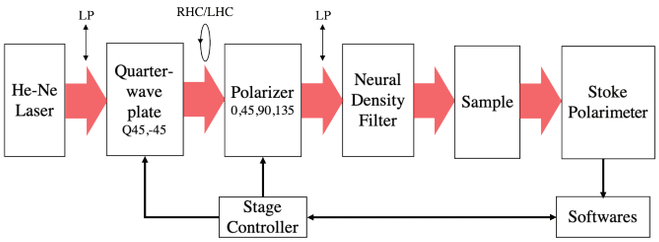

Fig. 1. The set-up of the optical system and measurement. A helium-neon (He-Ne) laser generates linearly polarized output that is characterized when passing through a series of optical elements. This light interacts with an anisotropic biological sample, then relays the optical information to a Stoke polarimeter. The nine effective optical parameters formulating linear birefringence, linear dichroism, circular birefringence, and circular dichroism are extracted by a software developed in Pham and Lo's laboratory. A stage controller rotates the quarter-wave plate and the polarizer to the exact angles needed during measurement. LP: linearly polarized. RHC/LHC: circularly right-hand-side/circularly left-hand-side.

Table 1. Symbols, ranges, and definitions of nine effective parameters.

Name	Symbol	Range	Definition(*)
Orientation angle of linear birefringence	α	$[0^0, 180^0]$	
Linear birefringence	β	$[0^0, 360^0]$	$2\pi(n_s - nf)l/\lambda_0$
Optical rotation or circular birefringence	γ	$[0^0, 180^0]$	$2\pi(n_- - n_+)l/\lambda_0$
Orientation angle of linear dichroism	θ_d	$[0^0, 180^0]$	
Linear dichroism	D	[0, 1]	$2\pi(\mu_s - \mu_f)l/\lambda_0$
Circular dichroism	R	[-1, 1]	$2\pi(\mu_- - \mu_+)l/\lambda_0$
Linear depolarization	e_1 and e_2	[-1, 1]	
Circular depolarization	e_3	[-1, 1]	

*n is the refractive index; μ is absorption coefficient; l is path length through a medium (thickness of material); and λ_0 is vacuum wavelength. Furthermore, subscript f and s represent the fast and slow linearly polarized waves, respectively, when neglecting the circular effects. Finally, + and - represent the right and left circularly polarized waves, respectively, when neglecting the linear effects.

The polarized light system included a helium-neon laser with a wavelength of 632 nm and power < 5 mW (Thorlabs, Inc., America), a quarter-wave plate (Thorlabs, Inc., America), a polarizer (Thorlabs, Inc., America), a detector (Thorlabs, Inc., America), two stage controllers (OptoSigma), a Stokes polarimeter (Thorlabs, Inc., America), and a computer. Fig. 2 illustrates the installation of the system. The He-Ne laser was placed at the first position; the quarter-wave plate and the polarizer were set at the second and third positions, respectively; the sample was at the fourth position; and the detector stood at the fifth position. A stage controller was used to automatically

control the lens rotation of the quarter-wave plate and the polarizer. A Stokes polarimeter analyzed signals received from the detector to provide six polarization angles. A computer displayed a graphic user interface of the stage controller, the Stokes polarimeter, and calculated a package of polarization angle data to extract nine effective parameters of the sample by an algorithm written on Matlab (MATLAB, The MathWorks, Inc.).

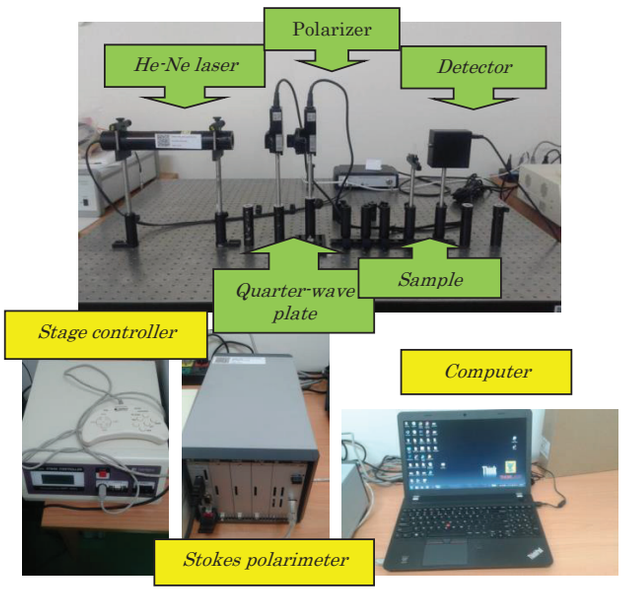

Fig. 2. Installation of the optical polarization system, including He-Ne laser, a quarter-wave plate, polarizer, sample holder, detector, stage controller, Stokes polarimeter, and computer.

Experiment design

To confirm the optimal condition for the research, a preliminary investigation was conducted. The design of the cellular model was based on the property of sample containers (standing quartz slides), available cell culture technique, and facilities. Specifically, we investigated cell densities, cell concentrations, medium volume, spreading area, and addictive substances that could enhance the adhesion of breast cancer cells to a 9 cm^2 area on the quartz slide. Preliminary investigation revealed the appropriate parameters for cell adhesion; meanwhile, preliminary results demonstrated the correspondingly approachable cell densities of the optical system.

The design for cell adhesion is illustrated in Fig. 3. One layer of fibronectin solution was coated on the quartz slide. It has been proved that this substance enhances the adhesion of cells to surfaces. After removing the excess solution, one layer of cell medium was placed above the dried fibronectin layer.

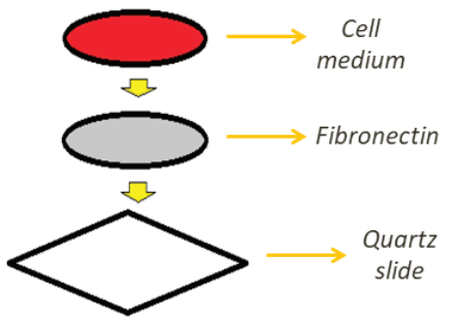

Fig. 3. Cell adhesion design that includes one layer of fibronectin and another layer of cells on quartz slide.

Table 2 presents appropriate parameters of the adhesive area, cell densities, the volume of medium applied to the adhesive area, and concentration of cells on the medium. It is noticeable that with the area of the quartz slide (9 cm^2), the suitable cell densities were 10^4 cells, 10^5 cells, and 10^6 cells, and the medium volume needed to be 500 µl. It was found that these numbers of cells, as well as the volume, resulted in a full two-dimensional cover for the area. Corresponding with cell densities and medium volume, cell concentrations should be 10^4 cells/500 µl, 10^5 cells/500 µl, and 10^6 cells/500 µl. For fibronectin, the suitable concentration and the appropriate volume per quartz slide were 10 µg/ml and 500 µl, respectively.

Table 2. Appropriate parameters for cell adhesion.

Parameter	Value
Adhesive area	9 cm^2
Cell density	10^4 cells/9 cm^2 10^5 cells/9 cm^2 10^6 cells/9 cm^2
Medium volume	500 µl/quartz slide
Cell concentration	10^4 cells/500 µl 10^5 cells/500 µl 10^6 cells/500 µl
Additive substance Concentration Volume	Fibronectin 10 µg/ml 500 µl/quartz slide
Incubating time	60 minutes

To confirm the study's findings, we also extended the model to 10^7 cells/500 µl. However, due to the mass amount of cells, we scaled the model 10 times, which was 10^6 cells/0.9 cm^2 with the equal volume of 50 µl for both fibronectin and cell medium.

Sample preparation

Cell culture: the BT474 human breast cancer cells were cultured in Dulbecco's modified Eagle medium (DMEM;

Gibco; Thermo Fisher Scientific, Inc., Waltham, MA, USA) supplemented with 10% fetal bovine serum (FBS) (Sigma-Aldrich), and 1% penicillin-streptomycin (PS) (Sigma-Aldrich). Cells were kept at 37^0C in humidified air with 5% CO_2.

Adhesion assays: firstly, the quartz plates were cleaned with alcohol 70^0 and distilled water, sterilized with ultraviolet light for 20 minutes, coated by filling with 500 µl of fibronectin in concentrations of 10 µg/ml, and incubated at 37^0C for one hour for the binding of the fibronectin. Then, the excess fibronectin was removed. While incubating fibronectin, we prepared a suspension of the cells with specific concentrations for the examination. Next, a volume of 500 µl was added for each concentration (that is 500 µl for 10^4 cells, 500 µl for 10^5 cells, and 500 µl for 10^6 cells) into each plate. The cells were allowed to adhere to the surface of the plate for one hour in a 37^0C-5% CO_2 incubator. Subsequently, the unbound cells were removed from the plate. The plates were put on Petri dishes and carried to the optical system in the Medical photonics laboratory - International University. For density 10^7, both the volume and the area were scaled down 10 times, which means 10^6 cells, volume of 50 µl, and an area of 0.9 cm^2. The process of the cell adhesion is illustrated in Fig. 4.

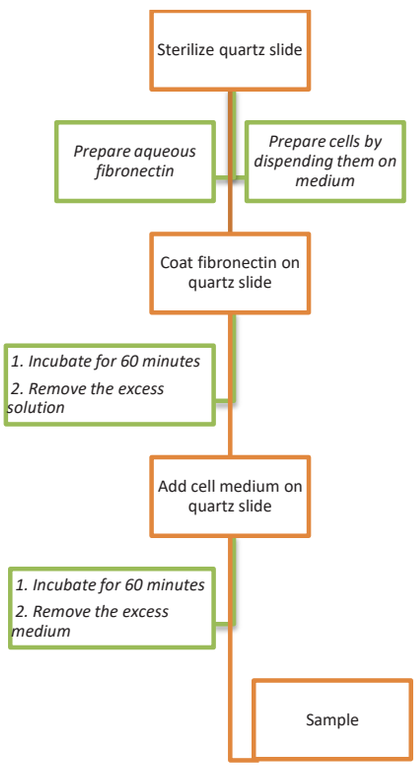

Fig. 4. Flowchart of the sample preparation process.

Figure 5 provides images of control samples and cell samples. To control the number of cells in a unit of area, the cell models were contained on transparent square slides kept in Petri dishes. A cell-counting technique was used in a unit of area under a modern microscope. From the results, we can determine the exact density of the cells in a sample. As can be seen, that density - 10^7 - was found in circles while control samples and other density samples covered the entire slide surface.

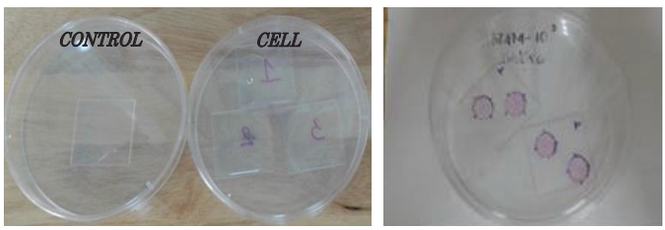

(A) **(B)**

Fig. 5. Control sample and cell samples after cell adhesion: control sample, density 10^4, density 10^5, density 10^6 (A), and density 10^7 (B).

It is noted that in Fig. 5, the control sample contains only one layer of fibronectin and the cell sample contains one layer of fibronectin and one layer of the cells with different specific concentrations.

Data acquisition and analysis

Six angles (i.e., right-hand-side and left-hand-side for circular polarization, 0^0, 45^0, 90^0, and 135^0 for linear polarization) were collected from three to five different points of each sample (i.e., control samples, samples of density 10^4, of 10^5, of 10^6, and 10^7). Six control samples; 12 samples of each density - 10^4, 10^5, 10^6; and six samples of density 10^7 were measured for the statistical significance.

Each data package of six polarization angles for each point on a sample was calculated by an algorithm written in a Matlab program (MATLAB, The MathWorks, Inc., Natick, Mass., United States) to extract nine effective parameters representing full optical properties of the measured samples.

Experimental results

Two-dimensional cellular models of breast carcinoma

This part presents the results of building cellular models for the investigation. Fig. 6 provides the images of four cell densities under the optical microscope (Nikon Corp., Minato, Tokyo, Japan) with the magnification of 40, 100, and 200. The photos were taken immediately after cell adhesion. From the photos, it was evident that the number of the cells was highest in photos of density 10^7, followed

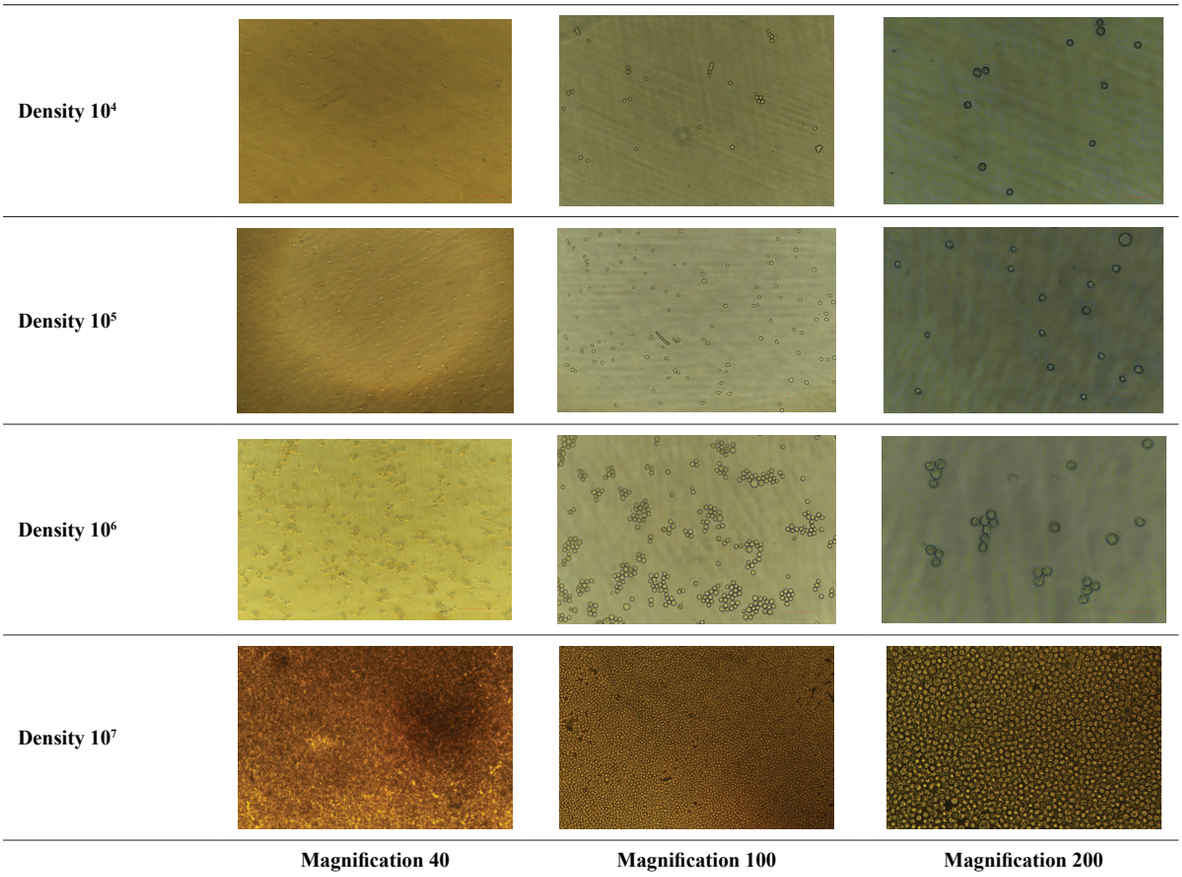

Fig. 6. Microscope images of BT474 after adhesion on quartz plates with different densities, i.e., 10^4, 10^5, 10^6, and 10^7, respectively.

by those of 10^6, lower in photos of density 10^5, and lowest in those of density 10^4. Alternatively, an increase in cell numbers corresponded with cell densities in the models. In addition, it is noticeable that density 10^7 was the maximum cell number entirely covering the surface of the quartz slide.

Effective optical parameters

This section reveals the values of effective optical parameters extracted from the investigated samples. Although 48 samples were built, only 40 samples were successfully measured. Nine effective parameters - orientation angle of linear birefringence (α), retardance or linear birefringence (β), optical rotation angle or circular birefringence (γ), orientation angle of linear dichroism (θd), linear dichroism (D), circular dichroism (R), degrees of linear depolarization (e1 and e2), and degree of circular depolarization (e3) - were extracted from a total of 40 samples by the polarized light system. Those samples included six each for control, density 10^4, and density 10^7, and 11 each for density 10^5 and density 10^6, respectively. Table 3 lists the sample number collected from each density to calculate the average value and standard deviation for effective optical parameters.

Table 3. A summary of all nine effective optical parameters of BT474 extracted using the decoupled analytical method.

Cell density	Nine effective optical parameters of BT474								
	α (deg)	*β (deg)*	*θd (deg)*	*D (deg)*	*γ (deg)*	*R (deg)*	*e1 (deg)*	*e2 (deg)*	*e3 (deg)*
10^4 cells/ml	121.55±20.542	0.934±0.4053	106.81±19.269	0.1446±0.0139	22.973±34.125	-0.0256±0.0647	1.0114±0.0124	-1.019±0.0468	3.5999±0.5799
10^5 cells/ml	146.3±23.219	1.6915±1.2625	93.936±30.066	0.1809±0.0201	7.7493±16.869	0.0152±0.0304	1.0133±0.089	-1.0194±0.0602	2.8651±1.0321
10^6 cells/ml	148.22±30.556	1.8298±1.3375	82.77±34.43	0.2518±0.0397	1.5173±4.0789	0.01±0.0355	0.974±0.0136	-1.009±0.3974	3.0097±0.7924

α: orientation angle of linear birefringence; β: linear birefringence; θd: orientation angle of LD; D: linear dichroism; γ: circular birefringence CB; R: circular dichroism CD; e1: linear depolarization; e2: linear depolarization; e3: circular depolarization.
N = 60 for each cell density.

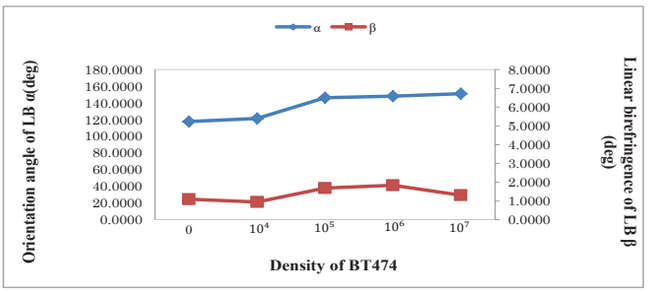

(A)

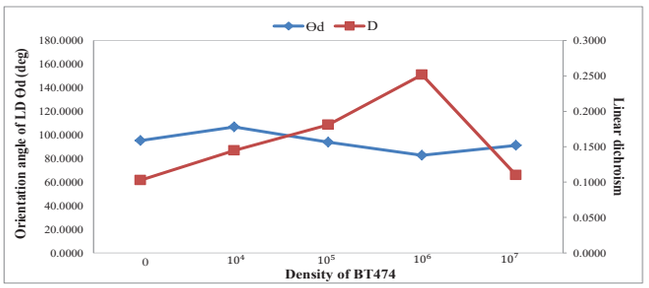

(B)

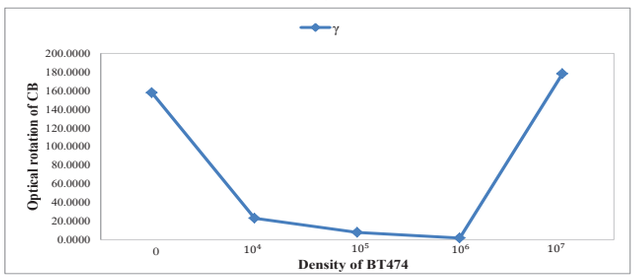

(C)

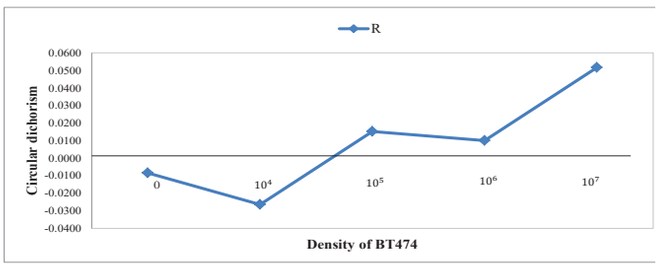

(D)

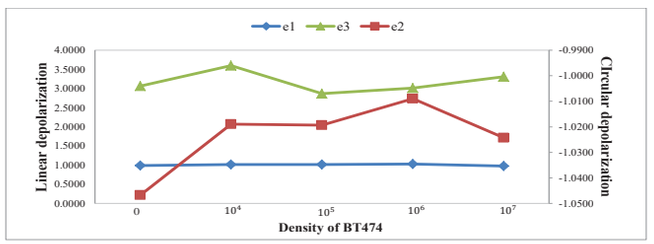

(E)

Fig. 7. Effective parameter values of five cell densities - density 0, density 10^4, density 10^5, density 10^6, and density 10^7. Orientation angle of linear birefringence values and linear birefringence (**A**), orientation angle of linear dichroism and linear dichroism linear (**B**), optical rotation or circular birefringence (**C**), circular dichroism (**D**), linear and circular depolarization (**E**).

Figure 7 illustrates the graphic results of extracted parameters for different cellular densities of BT474.

From the graphic illustration of Fig. 7, linear birefringence, linear dichroism, and circular birefringence values of three cell densities - 10^4, 10^5, and 10^6 - were plotted in Fig. 8 to illustrate the linear relationship of optical parameters with the increment of density of BT474. For example, Fig. 8 demonstrates that the orientation angle and linear birefringence of LB and optical rotation angle of CB increase linearly with the change of BT474 density, respectively. In Fig. 8B, the measured value of LD increases as the cell density increases. Meanwhile, the orientation angle of LD decreases when the BT474 density increases.

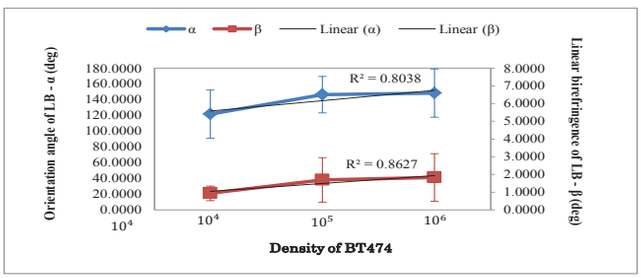

(A)

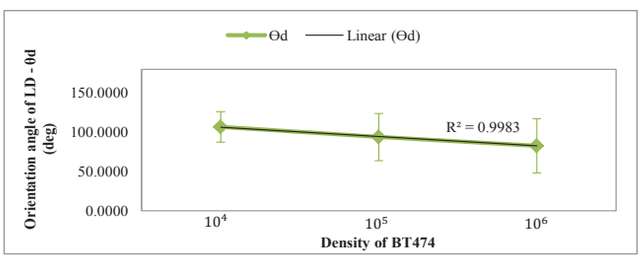

(B)

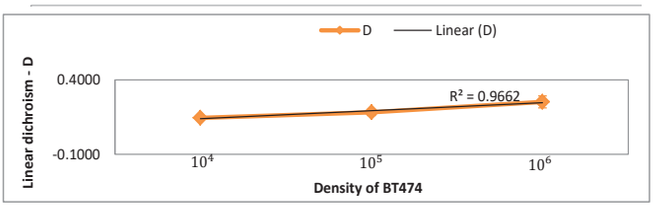

(C)

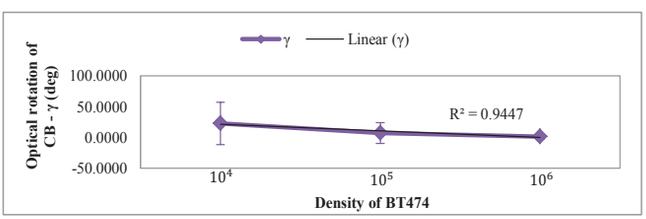

(D)

Fig. 8. Linear relationship between the range of cell density [10^4, 10^6] and orientation angle of linear birefringence and linear birefringence (A), orientation angle of linear dichroism (B), linear dichroism (C), circular birefringence (D).

Discussion and implementation

The possible explanation for the positive correlation between breast cancer cell densities and linear birefringence as well as linear dichroism is based on the work of Angelskaya, et al. [16]. In the study, the authors determined which substances in the tumour played the role of optical indicators of cancer changes in biological tissues. In particular, they concluded that two types of fluorophore in the tumour - NADH and collagen - resulted in an increase in linear birefringence and linear dichroism. However, the study focused on murine models and two types of cancer - prostate and esophageal - hence, there is a need for verification of breast cancer samples.

The negative correlation between the density range and circular birefringence was thought to be due to the decline in glucose concentration in cells when cancer developed. In other words, circular birefringence values decreased along with the rise of cell density. Meanwhile, there was no possible explanation for the decrease of linear birefringence's orientation angle corresponding with the exponential increase of cell density.

The lowest density (i.e., 10^4 cells/9 cm^2) reveals the potential of the polarized light system in early detecting breast cancer whereas the highest density (i.e., 10^7 cells/9 cm^2) reveals the threshold for both the two-dimensional model and the instrument. Specifically, that low density provides the sensitivity of the optical system in screening the malignant transition of mammary cells. In terms of the model, 10^7 cells are sufficient to build a two-dimensional layer on an area of 9 cm^2. In the context of the technique, concentration and thickness of the layer created by that cell density reach the threshold of the helium-neon laser (wavelength 632.5 nm, power < 5 mW). Alternatively, the laser is unable to penetrate through or will interact with the sample of that high density to provide good signals.

In terms of the cellular model, the cell adhesion process needs to be modified. Firstly, from microscopic photos (Fig. 1), BT474 did not spread well on the surface, and that made standard deviation of parameter values high. Additionally, the considerable discrepancy between cell numbers on the sample before and after removing floating cells requires cell counting for the sample. Besides, it is promising to extend the model to lower densities (i.e., 10^2 and 10^3 cells) for the primitive prognosis of breast cancer. When it comes to the technique, it can be seen that the values of the depolarization are out of the range. The reason is thought to come from the calculation. We suggest processing the data by alternative algorithms (i.e., genetic algorithm).

Conclusions

In conclusion, the optical system of a helium-neon laser (wavelength of 632 nm, power < 5 mW), a quarter-wave plate, polarizers, and a Stokes polarimeter utilizing the Mueller matrix decomposition and Stokes vector polarimetry was able to detect in-vitro mammary cancer through effective optical parameters. Specifically, there was a linear relationship between five parameters - linear birefringence (α and β), linear dichroism (θd and D), and circular birefringence (γ) - and the range of cell densities [10^4, 10^6]. The R-squared values were approximately over 0.8 and over 0.9. The system is promising for uncomplicated cancer diagnostics. In addition, the high threshold for two-dimensional cellular models was revealed to be 10^7 cells/9 cm^2 or 10^6 cells/0.9 cm^2.

ACKNOWLEDGEMENTS

The authors gratefully acknowledge the financial support provided to this study by the Vietnam National Foundation for Science and Technology Development (NAFOSTED) under grant number 103.03-2016.86.

The authors declare that there is no conflict of interest regarding the publication of this article.

REFERENCES

[1] J.G. Elmore, et al. (1998), "Ten-year risk of false positive screening mammograms and clinical breast examinations", *New England Journal of Medicine*, **338(16)**, pp.1089-1096.

[2] R.E. Bird, T.W. Wallace, B.C. Yankaskas (1992), "Analysis of cancers missed at screening mammography", *Radiology*, **184(3)**, pp.613-617.

[3] N. Obi, et al. (2011), "Impact of the quality assured mamma diagnostic (QuaMaDi) programme on survival of breast cancer patients", *Cancer Epidemiology*, **35(3)**, pp.286-292.

[4] M.F. Wood, et al. (2009), "Turbid polarimetry for tissue characterization", *European Conference on Biomedical Optics*, Optical Society of America.

[5] S.L. Jacques, J.R. Roman, K. Lee (2000), "Imaging superficial tissues with polarized light", *Lasers in Surgery and Medicine*, **26(2)**, pp.119-129.

[6] P. Sun, et al. (2014), "Mueller matrix decomposition for determination of optical rotation of glucose molecules in turbid media", *Journal of Biomedical Optics*, **19(4)**, Doi: 10.1117/1.JBO.19.4.046015.

[7] I. Ahmad, et al. (2015), "Ex vivo characterization of normal and adenocarcinoma colon samples by Mueller matrix polarimetry", *Journal of Biomedical Optics*, **20(5)**, Doi: 10.1117/1.JBO.20.5.056012.

[8] S. Alali, et al. (2014), "Assessment of local structural disorders of the bladder wall in partial bladder outlet obstruction using polarized light imaging", *Biomedical Optics Express*, **5(2)**, pp.621-629.

[9] T.T.H. Pham, Y.L. Lo (2012a), "Extraction of effective parameters of anisotropic optical materials using a decoupled analytical method", *Journal of Biomedical Optics*, **17(2)**, Doi: 10.1117/1.JBO.17.2.025006.

[10] T.T.H. Pham, Y.L. Lo (2012b), "Extraction of effective parameters of turbid media utilizing the Mueller matrix approach: study of glucose sensing", *Journal of Biomedical Optics*, **17(9)**, Doi: 10.1117/1.JBO.17.9.097002.

[11] Hien Thi-Thu Pham, Anh Le-Trang Nguyen, Toi-Van Vo, Khon-Chan Huynh, Quoc-Hung Phan (2018), "Optical parameters of human blood plasma, collagen, and calfskin based on the Stokes-Mueller technique", *Applied Optics*, **57(16)**, pp.4353-4359.

[12] B.L. Parsons (2008), "Many different tumor types have polyclonal tumor origin: evidence and implications", *Mutation Research/Reviews in Mutation Research*, **659(3)**, pp.232-247.

[13] N.F. Boyd, et al. (2010), "Breast tissue composition and susceptibility to breast cancer", *Journal of the National Cancer Institute*, **102(16)**, pp.1224-1237.

[14] B. Weigelt, J.S. Reis-Filho (2009), "Histological and molecular types of breast cancer: is there a unifying taxonomy?", *Nature Reviews Clinical Oncology*, **6(12)**, pp.718-730.

[15] D.L. Holliday, V. Speirs (2011), "Choosing the right cell line for breast cancer research", *Breast Cancer Research*, **13(4)**, p.215, Doi: 10.1186/bcr2889.

[16] A. Angelskaya, et al. (2013), "Manifestations of linear dichroism changes in cancer biotissues", *Romanian Reports in Physics*, **65(3)**, pp.1052-1062.